

Störmer problem restricted to a spherical surface

This content has been downloaded from IOPscience. Please scroll down to see the full text.

2015 Eur. J. Phys. 36 055009

(<http://iopscience.iop.org/0143-0807/36/5/055009>)

View the [table of contents for this issue](#), or go to the [journal homepage](#) for more

Download details:

IP Address: 134.117.10.200

This content was downloaded on 10/07/2015 at 11:41

Please note that [terms and conditions apply](#).

Störmer problem restricted to a spherical surface

Emilio Cortés¹ and David Cortés Poza²

¹ Departamento de Física, Universidad Autónoma Metropolitana Iztapalapa, PO Box 55-534, México D.F. 09340, México and Member of SNI, México

² Center for Intelligent Machines, McGill University, Montreal, Canada

E-mail: emil@xanum.uam.mx

Received 19 January 2015, revised 7 April 2015

Accepted for publication 17 April 2015

Published 26 June 2015



Abstract

In order to analyse in full detail the dynamics of a charged particle in the field of a magnetic dipole, we propose to study the restricted motion of the particle in a spherical surface with the dipole at its centre. This model can be considered as the classical non-relativistic Störmer problem within a sphere, and although this problem no longer represents the real Störmer problem, it shows the complex behaviour of this magnetic field through the classical dynamics equations that can be formally integrated. We start from a Lagrangian approach which allows us to analyse the dynamical properties of the system, such as the role of a velocity dependent potential, the symmetries and the conservation properties. We derive the Hamilton equations of motion, which in this restricted case can be reduced to a quadrature. From the Hamiltonian function we find, for the polar angle, an equivalent one-dimensional system of a particle in the presence of an effective potential. This equivalent potential function, which is a double well potential, allows us to get a clear description of the dynamics of the system. Then we obtain, by means of numerical integration, different plots of the trajectories in three-dimensional graphs in the sphere. This restricted case of the Störmer problem is still nonlinear, with complex and interesting dynamics and we believe that it can offer the student a better grasp of the subject than the general three-dimensional case.

Keywords: Störmer problem, charge in a dipole field, Lagrangian dynamics, Hamiltonian dynamics

1. Introduction

The motion of a charged particle in a magnetic field has been of interest since the discovery of cosmic rays, at the beginning of the twentieth century. This problem was studied extensively

by Carl Störmer [1] for many years, and it is now called Störmer problem. As the cosmic rays are composed of energetic subatomic particles, the particle dynamics belong to the relativistic domain. See an early review [2]. The relevance of the system was the modelling of the Aurora Borealis phenomenon and later, in the middle of the last century, it received an impulse with the discovery of the Van Allen belts. During the first half of the last century, physicists and mathematicians, considering the Earth's magnetic field as a bar magnet, as an approximation, they studied the problem of describing the dynamics of a charge in a magnetic dipole field. Henri Poincaré [3] was able solve the motion of charged particles near an isolated magnetic pole, showing that they spiraled around field lines and they were repelled from regions of strong field (the poles).

Many analytical and numerical models have been developed to study this problem. Special interest has been focused in the study of trapped orbits [1]–[4], among the many different classes of orbits that depend on the initial conditions. The general problem has three degrees of freedom and, since the magnetic field of the dipole has an axis of symmetry and the energy is conserved, two constants of motion are readily identified. After decades of searching for an additional integral of motion, it was concluded that the problem is not integrable. In fact, Dragt A J and Finn J M 1976 [5] explicitly prove the nonintegrability of the problem of trapped charged particle motion in a magnetic dipole field. Actually, it has been shown that the problem is chaotic [5]–[7].

In the present work we tackled the restricted case of the classical problem of a charge constrained to a spherical surface, interacting with the magnetic dipole at the centre of the sphere. Although the model can no longer be applied to the study of the cosmic radiation and the Earth's field, we believe that it may illustrate the complex dynamics of a point charge in the field of a magnetic dipole. We see explicitly how in this two-dimensional system, the equations of motion are formally integrable in its polar and azimuthal angular variables and we are able to find for the polar angle a one-dimensional equivalent dynamical system with an effective potential function. We obtain also a formal solution of the azimuthal angle in terms of the polar angle, as well as the presence of loops in the paths in the spherical domain.

The study of this electromagnetic phenomenon involves two different fields of physics, in one hand we have the interaction of a moving charge with a static electromagnetic field and in the other hand its dynamical description takes us into classical mechanics. The magnetic interaction of this system is usually covered in an advanced undergraduate course of electromagnetism, however the dynamical analysis of the charged particle is more suitable for the graduate level of analytical mechanics. This work can be a complementary material in both courses, within a seminar or as a student presentation assignment.

We expect that with this analysis the student will observe that establishing the Lagrangian function is the starting point which connects the electromagnetic system with its classical dynamics description. The Lagrangian and Hamiltonian dynamics of the system turns out to be by itself an interesting and not very usual application of the concepts of advanced mechanics. The student will also appreciate the complex behaviour of a charge in the field of a magnetic dipole. We believe that the student will gain a better insight into some of the dynamical properties associated also with the non-restricted Störmer problem. Among these properties we can mention that the velocity-dependent potential energy function does not change the kinetic energy which, in this case, is the same as the Hamiltonian function, the latter being a constant of motion. It is also observed that the canonical momentum associated with the azimuthal angle is another constant of motion, and it is not the angular momentum. We have not found in the literature the study of this restricted Störmer problem.

The work is organized in the following way: in section 2 we establish the problem through the Lagrangian approach and discuss some important properties of the dynamical

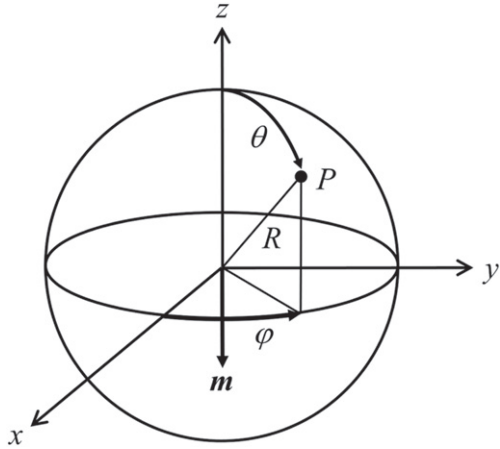


Figure 1. Spherical surface where the charge is constrained. The magnetic dipole is located at the centre of the sphere, with its dipole moment pointing along the negative z axis. We will use (R, θ, φ) as the spherical coordinates, and (x, y, z) as the rectangular coordinates of a point P .

system. In section 3 we derive the Hamilton equations and show that they are formally integrable. In section 4 we analyse the dynamics in the polar angle variable and find the equivalence of the system with a one-dimensional problem with an effective double well potential. We discuss different properties of the paths according to this framework. In section 5, from a numerical integration of the equations of motion, we present 3D plots of different paths to compare with the analytical results and illustrate the different motion regimes that this dynamical system exhibits. In section 6 we study the critical points of the equations of motion for $\dot{\theta}$ and $\dot{\varphi}$ and discuss the turning points and the presence of loops in the spherical surface, as well as other properties of the path with respect to the azimuthal motion. Finally in section 7 we present our conclusions.

2. Dynamical system

We will use spherical coordinates, R, θ, φ , to represent the position of the particle at the point P , we set R constant, and we just have two coordinates, the polar and azimuthal angles, see figure 1. We set the magnetic dipole in the centre of the sphere with its magnetic dipole moment \mathbf{m} pointing downwards. We define M as the mass of the particle, the axes x and y are located in the equatorial plane and z is the vertical or symmetry axis. As we know, with this selection we have the south magnetic pole in the direction of the upper hemisphere. This is the case of the magnetic Earth's field. The magnetic vector potential is then expressed as

$$\mathbf{A} = \frac{\mu_0 \mathbf{m} \times \mathbf{a}_R}{4\pi R^2}, \quad (1)$$

where μ_0 is the magnetic permeability of vacuum, and \mathbf{a}_R is a unit vector in the radial direction.

From figure 1 we can write the vector \mathbf{A} in the form

$$\mathbf{A} = \frac{-\mu_0 \mathbf{m} \sin \theta \mathbf{a}_\varphi}{4\pi R^2}, \quad (2)$$

where \mathbf{a}_φ is a unit vector in the azimuthal direction. Now, instead of starting with the Lorentz force, we prefer to follow the Lagrangian formalism due to the fact that from this, we are able not only to derive more directly the equations of motion of the charge, but we can also obtain some important dynamical features like the symmetries and the conserved quantities. The Lagrangian of the system has the form

$$L = K - U, \quad (3)$$

where K is the kinetic energy of the particle and U is a velocity dependent potential which it is shown [8] to be

$$U = -q \mathbf{v} \cdot \mathbf{A}, \quad (4)$$

where \mathbf{v} is the velocity vector and q is the charge of the particle. In spherical coordinates we have

$$\mathbf{v} = R \dot{\theta} \mathbf{a}_\theta + R \sin \theta \dot{\varphi} \mathbf{a}_\varphi, \quad (5)$$

where we use the unit vectors \mathbf{a}_θ and \mathbf{a}_φ .

Substituting equations (2) and (5) in (4) we have

$$U = k \dot{\varphi} \sin^2 \theta, \quad (6)$$

where we are defining

$$k = \frac{q \mu_0 m}{4\pi R}. \quad (7)$$

From equation (5) the kinetic energy is written as

$$K = \frac{1}{2} MR^2 (\dot{\theta}^2 + \dot{\varphi}^2 \sin^2 \theta). \quad (8)$$

Then the Lagrangian equation (3) is written as

$$L = \frac{1}{2} MR^2 (\dot{\theta}^2 + \dot{\varphi}^2 \sin^2 \theta) - k \dot{\varphi} \sin^2 \theta. \quad (9)$$

The canonical conjugate momenta are defined as

$$p_\theta = \frac{\partial L}{\partial \dot{\theta}} = MR^2 \dot{\theta}, \quad (10)$$

and

$$p_\varphi = \frac{\partial L}{\partial \dot{\varphi}} = [MR^2 \dot{\varphi} - k] \sin^2 \theta. \quad (11)$$

We observe that the term defined by

$$\eta \equiv MR^2 \dot{\varphi} \sin^2 \theta, \quad (12)$$

is the component of the angular momentum of the particle along the symmetry axis, z . Since φ is an ignorable coordinate due to the symmetry, then p_φ , the conjugate momentum associated with this angle, is a constant of motion, but it is not an angular momentum; it has a term due to the magnetic field, that does not depend on a velocity. Then we get our first conserved quantity

$$p_\varphi = \eta - k \sin^2 \theta = \text{const.} \quad (13)$$

The Hamiltonian of the system is defined in this case as

$$H = \dot{\theta} p_\theta + \dot{\varphi} p_\varphi - L. \quad (14)$$

From equations (10) and (11), first we write the function H in terms of angles and velocities, after cancelling two terms we obtain

$$H = \frac{1}{2} MR^2 \left(\dot{\theta}^2 + \dot{\varphi}^2 \sin^2 \theta \right), \quad (15)$$

and we find that H is just the kinetic energy of the particle. We observe that the contribution of the magnetic field is implicit in the second term of this expression. As we know, the Hamiltonian here is another conserved quantity because L does not depend explicitly on time. So this means that the kinetic energy is conserved, therefore the speed of the particle is also a constant. We recall that a static magnetic field does not produce work on a moving charge, although in this case it does produce a torque. The velocity dependent potential given by equation (4) does not contribute to the energy of the particle.

We identify two symmetries in the system, which means that the Lagrangian is invariant under translations in the time t and in the azimuthal angle φ . See Noether theorem [9]. These symmetries correspond to the two constants of motion, the Hamiltonian or kinetic energy and the generalized momentum p_φ . The angular momentum for arbitrary initial conditions is not conserved; we observe here that as the number degrees of freedom does not exceed the number of constants of motion, then the equations of motion are formally integrable. We point out that in the non-restricted Störmer problem, where also the radial distance is variable, we have three degrees of freedom but again the same two conserved quantities. As we mention in the introduction, the three-dimensional problem is not solvable, and actually it happens to be chaotic [5]–[7].

Now we can write the Hamiltonian again from equations (10) and (11) in terms of the coordinates and momenta and obtain

$$H = \frac{1}{2MR^2} \left[p_\theta^2 + \frac{(p_\varphi + k \sin^2 \theta)^2}{\sin^2 \theta} \right]. \quad (16)$$

Then, in the second term of the last expression, we explicitly see that the contribution of the magnetic field to the kinetic energy of the particle occurs in the azimuthal motion, and it is just a function of the θ coordinate. Using the integral of motion given by equation (16) we can write

$$p_\theta = \pm \left(2MR^2 H - \frac{\eta^2}{\sin^2 \theta} \right)^{\frac{1}{2}}. \quad (17)$$

Substituting in equation (11) we obtain a quadrature

$$t = \pm MR^2 \int_{\theta_0}^{\theta} \left[2MR^2 H - \frac{\eta^2}{\sin^2 \theta} \right]^{-\frac{1}{2}} d\theta. \quad (18)$$

The function $\theta(t)$ can be obtained formally from the last equation, and then equation (11) can be integrated to obtain the function $\varphi(t)$. However, the integral given by equation (18) cannot be found in terms of analytic functions and a numerical procedure would be necessary.

Instead, given that equation (18) is multivalued, it will be more convenient to integrate the Hamilton equations numerically, which are going to be derived next.

3. Hamilton equations

From the Hamiltonian, equation (16) and using equation (12), we write the Hamilton equations; first we have

$$\dot{\theta} = \frac{\partial H}{\partial p_\theta} = \frac{p_\theta}{MR^2}, \quad (19)$$

$$\dot{\varphi} = \frac{\partial H}{\partial p_\varphi} = \frac{\eta}{MR^2 \sin^2 \theta}. \quad (20)$$

These two equations could have already been written from equations (10)–(12). The other two equations are

$$\dot{p}_\theta = -\frac{\partial H}{\partial \theta} = \frac{\eta}{MR^2 \sin^2 \theta} [\eta \cot \theta - k \sin 2\theta], \quad (21)$$

$$\dot{p}_\varphi = -\frac{\partial H}{\partial \varphi} = 0. \quad (22)$$

The last equation was of course already given by equation (13). We point out that the two poles (north and south) are singular points, see equations (20) and (21). We assume that the polar angle is restricted to the open interval between 0 and π , which is justified as long as the trajectory of the particle does not go directly into any of the poles. Actually, we see in equation (20) that $\dot{\varphi}$ grows indefinitely when the particle approaches the poles, so the azimuthal angular momentum also increases and this reduces the chances for the particle reaching these two points. As a matter of fact, as we will see in the next section, the particle is subject to a repulsive effect when it approaches the poles [3]. We see in the Hamilton equations, that equations (19), (20) and (16) can be integrated formally to give a function $\varphi(\theta)$:

$$\varphi(\theta) = \pm \int_{\theta_0}^{\theta} \frac{\eta d\theta}{\sin^2 \theta \sqrt{2MR^2 - \eta^2 \csc^2 \theta}}. \quad (23)$$

This integral cannot be expressed in terms of known functions, so a numerical method would be required. This means that a full analytical solution of the Hamilton equations is not possible. On the other hand, equations (19) and (21) constitute a coupled system of equations in the variable θ . If we divide equation (21) by equation (19) we can integrate and obtain an analytical expression for $p_\theta(\theta)$, we can write

$$\begin{aligned} p_\theta(\theta) &= \pm \left[p_{\theta 0}^2 + 2 \int_{\theta_0}^{\theta} \eta (\eta \cot \theta - k \sin 2\theta) \csc^2 \theta \right]^{\frac{1}{2}} d\theta \\ &= \pm \left[p_{\theta 0}^2 + k^2 (\cos^2 \theta - \cos^2 \theta_0) - p_\varphi^2 (\cot^2 \theta - \cot^2 \theta_0) \right]^{\frac{1}{2}}, \end{aligned} \quad (24)$$

where $p_{\theta 0}$ stands for $p_\theta(0)$.

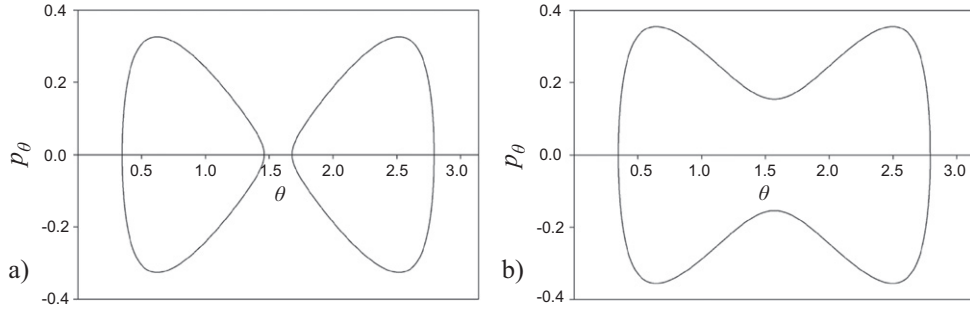


Figure 2. The phase space diagram of p_θ versus θ for two different values for the constant p_ϕ . In (a) $p_\phi = 0.34 k$ and in (b) $p_\phi = 0.36 k$.

4. The phase space (θ, p_θ) and the effective potential

4.1. The phase space

We see that the domain of function $p_\theta(\theta)$ in equation (24) may exclude some intervals of the angle θ , depending on the values of the parameters. In figure 2 we plot this function from 0 to π , with, $R = 10$ and $k = 0.5$, the initial values $p_\theta(0) = 0$, $\theta(0) = \frac{\pi}{9}$ and for the constant p_ϕ we chose two values: $p_\phi = 0.34 k$, for which the curve exhibits two separated islands, and $p_\phi = 0.36 k$ for which one obtains a simple closed curve; all the values are in arbitrary units. Here we point out that the initial values $p_\theta(0)$ and $\theta(0)$ determine the energy of the system, see equation (16). We clearly observe a symmetry with respect to the equator, $\theta = \frac{\pi}{2}$. This curve is similar to what is obtained in a ‘bistable potential’, whose phase space diagram can consist of one single closed curve or two closed curves, depending on the energy value. We point out here that the projection of the particle trajectory on the (θ, p_θ) plane is always a closed path. The path in the spherical surface in general will be non-closed due to the azimuthal motion. In other words, in the three-dimensional space $(\theta, p_\theta, \varphi)$ the plot of the trajectory will have a helicoidal shape which lies on the surface of a torus.

4.2. The effective potential

Let us write again equation (16) for the Hamiltonian or kinetic energy

$$H = \frac{1}{2MR^2} \left[p_\theta^2 + (p_\phi + k \sin^2 \theta)^2 \csc^2 \theta \right]. \quad (25)$$

We observe that the second term of this equation is the contribution of the azimuthal degree of freedom to the kinetic energy and, as we said, it does not depend on a velocity, but just on the polar coordinate. Then we can think in an equivalent one-dimensional problem, where the first term is the kinetic energy and the second one is an ‘effective potential’

$$V_{\text{eff}}(\theta) = \frac{1}{2MR^2} (p_\phi + k \sin^2 \theta)^2 \csc^2 \theta. \quad (26)$$

Now we make a plot of this potential, see figure 3, with the following values for the parameters: $M = 2$, $R = 10$, $k = 0.5$ (in arbitrary units) and two different values for the

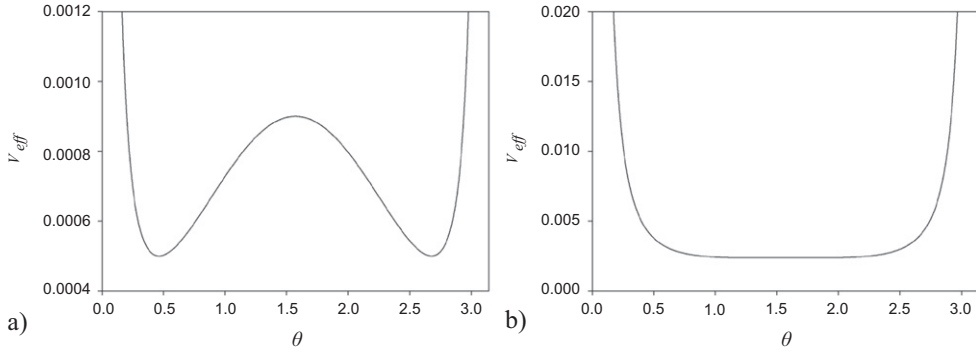


Figure 3. The effective potential of the equivalent one-dimensional system in the variable θ , for two different values of the constant p_ϕ . In (a) $p_\phi = 0.2 k$ and in (b) $p_\phi = 0.95 k$.

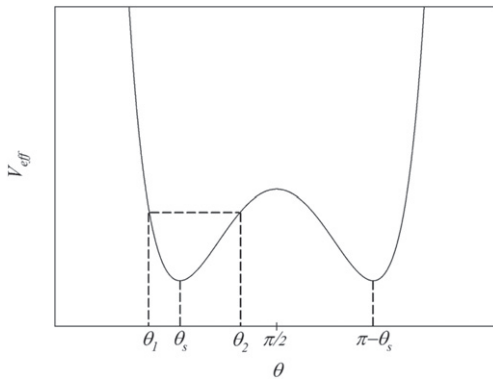


Figure 4. The effective potential showing its extreme values and turning points.

constant: $p_\phi = 0.2k$ and $p_\phi = 0.95k$. It is effectively a symmetric bistable potential (or a single well), with its middle point in $\theta = \frac{\pi}{2}$ (the equator).

There are some important features of our system that can be deduced from this potential. First we can appreciate a repulsive effect when the particle approaches the poles [3]. Then we can show from the equation (26) that for $|p_\phi| \geq k$ the maximum in the potential disappears and we will have only one well between the two poles $\theta = 0$ and $\theta = \pi$. So we have as a condition for the bistability,

$$|p_\phi| < k \quad (27)$$

Now, in the presence of the double well, see figure 4, we have two stable equilibrium points θ_s and $\pi - \theta_s$, and one unstable equilibrium point at $\theta = \frac{\pi}{2}$. These three points correspond to horizontal paths ($\theta = \text{const}$). On each one of the wells (hemispheres) we observe the presence of two turning points, θ_1 and θ_2 , where $p_\theta = 0$ and then the total energy is given by the value of V_{eff} at this level. If the total energy is big enough, the particle will cross the barrier and it will travel periodically from one hemisphere to the other.

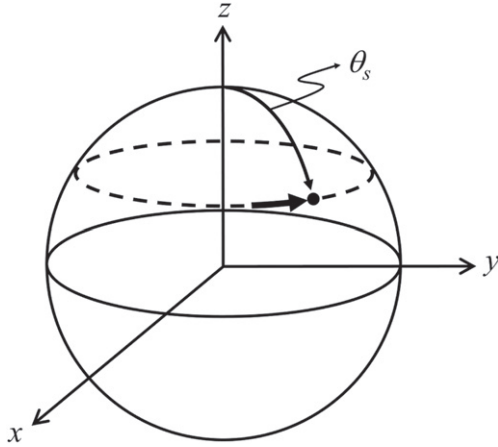


Figure 5. Horizontal closed path defined by $\theta = \theta_s$.

From equation (26) we can take the derivative to identify its extreme values, and using equation (13), we have

$$V'_{\text{eff}} = \frac{\eta \csc^3 \theta}{MR^2} \cos \theta (2k \sin^2 \theta - \eta) = 0. \quad (28)$$

We have three possible solutions of this equation:

- (a) $\eta = 0$,
- (b) $\eta = 2k \sin^2 \theta$,
- (c) $\cos \theta = 0 \rightarrow \theta = \frac{\pi}{2}$.

In (a), the first solution, from equation (12) we have $\dot{\phi} = 0$ and, since we are on an extreme point of the potential then $\dot{\theta} = 0$, which means that the particle is at rest at any of the two stable equilibrium points. The corresponding angle θ_s is obtained from equation (13).

$$\theta_s = \sin^{-1} \left(\frac{-p_\phi}{k} \right)^{\frac{1}{2}}. \quad (29)$$

(We take the positive sign of the square root, because of the domain $0 < \theta < \pi$). Here we point out that the constant conjugate momentum p_ϕ has to be negative as a necessary condition for the particle to be at rest. We notice that this conjugate momentum is not zero even when the particle is in a static equilibrium; this is due to the fact that from the definition of this quantity in equation (11), it contains a term that depends just in the polar angle and not in a velocity.

In (b), the second solution, from equations (12) and (13) we have:

$$p_\phi = k \sin^2 \theta, \quad (30)$$

$$\dot{\phi} = \frac{\eta}{MR^2 \sin^2 \theta_s} = \frac{2k}{MR^2} \quad (31)$$

Here $\theta_s = \sin^{-1} \left(\frac{p_\phi}{k} \right)^{\frac{1}{2}}$ (we take the positive sign due to the domain $0 < \theta < \pi$). The conjugate momentum p_ϕ , has to be positive as a necessary condition for this stationary value. This yields the two values of the minimum points in the bistable potential, see figure 4.

$$\theta_1 = \theta_s \quad (32)$$

$$\theta_2 = \pi - \theta_s \quad (33)$$

Then we have a horizontal closed trajectory at an angle θ_s , see figure 5.

We see in equation (31) that the angular velocity $\dot{\varphi}$ turns out to be independent of the polar angle and then the period for any of these horizontal paths is the same and has the value

$$T_h = \frac{\pi M R^2}{k}. \quad (34)$$

We note that the speed for these different horizontal paths depends on the angle θ_s ,

$$v = \dot{\varphi} R \sin \theta_s. \quad (35)$$

We recall here that the kinetic energy of the particle is a constant, once the parameters and initial values are given. So, the speed of the particle is also a constant for the given value of the angle θ_s in last equation. However, an interesting result is that the period for all these horizontal paths is the same for any polar angle different from $\frac{\pi}{2}$, a case that we will examine next.

In (c), the third solution ($\theta = \frac{\pi}{2}$) corresponds to an equatorial trajectory. From equation (20) the azimuthal angular velocity is then

$$\dot{\varphi} = \frac{1}{MR^2} (p_\phi + k) = \text{const.} \quad (36)$$

We observe here that as $-k < p_\phi < k$ then the particle always travels to the east as long as we are in this ‘bistable regime’. We see that among all the horizontal closed trajectories, only those located in the equator ($\theta = \frac{\pi}{2}$), can have different angular velocities depending on the value of the constant p_ϕ . For any other value of the polar angle the angular velocity is given by the equation (31).

4.3. Horizontal bands

Now, when $\theta(t)$ is changing, the path of the particle can be trapped in any of the two wells, if the condition of bistability is satisfied, which is $|p_\phi| < k$, and the energy is smaller than the maximum of the potential. We chose $p_\theta(0) = 0$ (or some small value) and we set for the energy (obtained by the value of $\theta(0)$ according to equation (26)), a value for which the potential is not bigger than the barrier height. What we have here is that the particle is trapped in a horizontal band defined by two values θ_1 and θ_2 which have the same potential energy, see the potential in figure 4 and the paths obtained numerically, figures 6(a)–(c). We point out that if $|p_\phi| \geq k$ then the effective potential has just one well and the path will still be within a band, which crosses the equator. See figure 3(b).

5. Spherical 3D plots

We can compare the analytical results to those obtained from the numerical integration of the Hamilton equations, equations (19)–(21), using a fourth order Runge–Kuta algorithm, which is going to be used for all the graphs in the rest of this work. We obtain some 3D graphs for

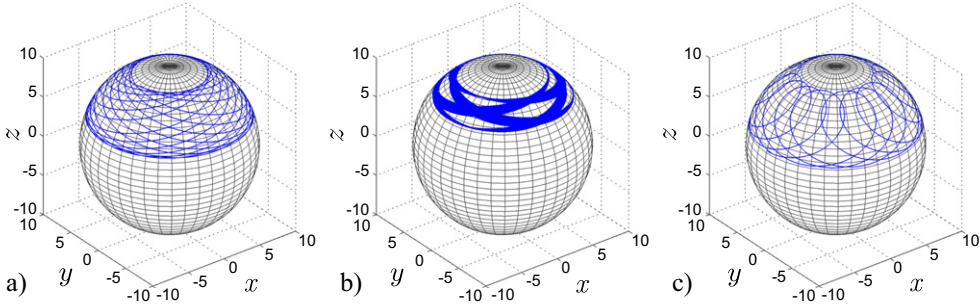


Figure 6. Three different paths in the sphere in a 3D plot. In all the cases the paths are trapped in a band between two polar angles in the northern hemisphere. In (a) we set $\theta_0 = \frac{\pi}{4}$, $p_{\theta 0} = 0$ and $p_\phi = 0.394$ in (b) we set $\theta_0 = \frac{\pi}{3}$, $p_{\theta 0} = 0$ and $p_\phi = 0.394$ in (c) we set $\theta_0 = \frac{75}{180}\pi$, $p_{\theta 0} = 0$ and $p_\phi = -0.394$. (In arbitrary units).

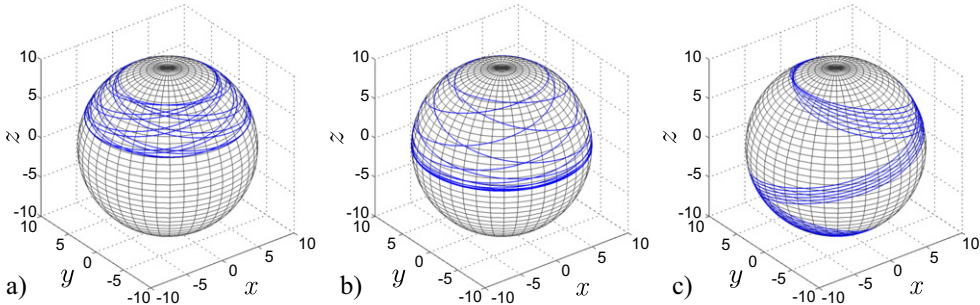


Figure 7. Three paths with different initial values of the moment $p_{\theta 0}$. In the three paths we set $\theta_0 = 0.6$ rad, $p_\phi = 0.5k$. In (a) $p_{\theta 0} = 0.1$ for which the particle remains in the northern hemisphere; in (b) $p_{\theta 0} = 0.191725$, for which the path reaches the equatorial limit and in (c) $p_{\theta 0} = 0.2525$, here the particle crosses and moves periodically between the two hemispheres.

the particle trajectory in different regimes. We are choosing for the mass and radius $M = 2$ and $R = 10$ respectively, and $k = 0.5$, in arbitrary units.

In figures 6(a)–(c) we see some paths trapped in a band in the northern hemisphere. In all of them we set $p_{\theta 0} = 0$ and different values of θ_0 and the constant p_ϕ . In figures 7(a)–(c) we present three different plots with the same initial polar angle $\theta_0 = 0.6$ rad and different values of $p_{\theta 0}$. In figure 7(a) we set $p_{\theta 0} = 0.1$, in figure 7(b) we set $p_{\theta 0} = 0.191725$ and in figure 7(c) we set $p_{\theta 0} = 0.25$. In figure 7(b) we notice what can be called the equatorial limit of a path, where $p_\theta = 0$ is a turning point. In figure 7(c) the path crosses the equator and goes periodically from one hemisphere to the other.

6. Critical points: turning points and loops

In the previous section we have studied the behaviour of the dynamics of the polar angle coordinate, and we already described the critical points $\dot{\theta} = 0$, as the turning points in the effective potential plot. Now, we want to consider the dynamics of the azimuthal angle. We

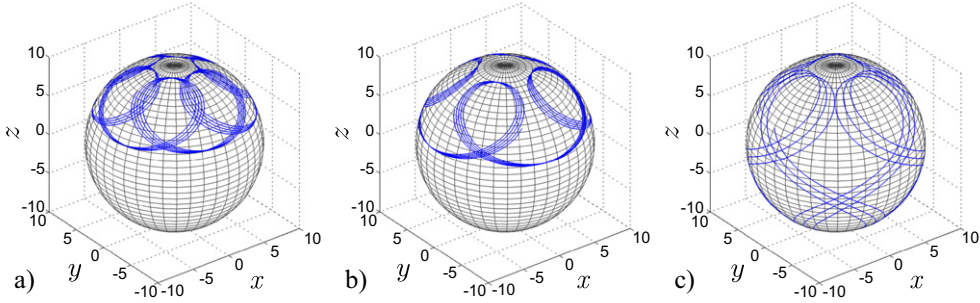


Figure 8. We have three different paths that, according to the condition given by equation (39), exhibit the presence of loops in the spherical surface. In (a) we have $\theta_0 = \frac{\pi}{6}$, $p_{\theta 0} = 0.34$ and $p_\varphi = -0.25 k$. In (b) we have $\theta_0 = \frac{\pi}{4}$, $p_{\theta 0} = 0.3$ and $p_\varphi = -0.3 k$. In (c) we have $\theta_0 = \frac{\pi}{3}$, $p_{\theta 0} = 0.3$ and $p_\varphi = -0.3 k$.

want to see what is the behaviour of the equation (20) in the critical points, where the angular velocity $\dot{\varphi}$ vanishes. We see that if the azimuthal angular velocity is zero and if the two poles are excluded, then the azimuthal angular momentum is zero,

$$\eta = 0, \quad (37)$$

which from equation (13) we obtain

$$\sin \theta \equiv u = + \sqrt{-\frac{p_\varphi}{k}}. \quad (38)$$

As the domain of the polar angle is $0 < \theta < \pi$, then we exclude the negative sign in the previous equation. This result means that the condition $\dot{\varphi} = 0$ requires the condition

$$-k < p_\varphi < 0. \quad (39)$$

In this angle, equation (38), the sign of the azimuthal velocity changes. The angle is the same as the minimum of the potential given in equation (29), and it is located between the angles θ_1 and θ_2 , which are the turning points, where $\dot{\theta} = 0$, see figure 4. As $\dot{\varphi}$ varies periodically with θ , see equation (11), then we have the presence of loops in the trajectory. So we see that there is an out-of-phase synchronization between $\dot{\theta}$ and $\dot{\varphi}$; so this means that under this regime, given by the inequality (39), we will have the presence of loops in the (θ, φ) surface, as we can see in figure 8. We want to make a remark about these paths in the spherical surface: we could have in some paths the presence of ‘pseudo-loops’, when the apparent loops (even if they are narrow) go around any one of the poles, see figure 7(c); in these cases $\dot{\varphi}$ does not change its sign. In other words, the authentic loops do not enclose any pole of the sphere. We observe that all the paths of figure 7 are obtained for a positive value of p_φ which is different to the condition in equation (39).

Now, with respect to the direction of the azimuthal motion of the particle we can take equations (13) and (20) and write for the angular velocity

$$\dot{\varphi} = \frac{p_\varphi + k \sin^2 \theta}{MR^2 \sin^2 \theta}. \quad (40)$$

From this equation we can classify different trajectories, according to the azimuthal direction of the motion,

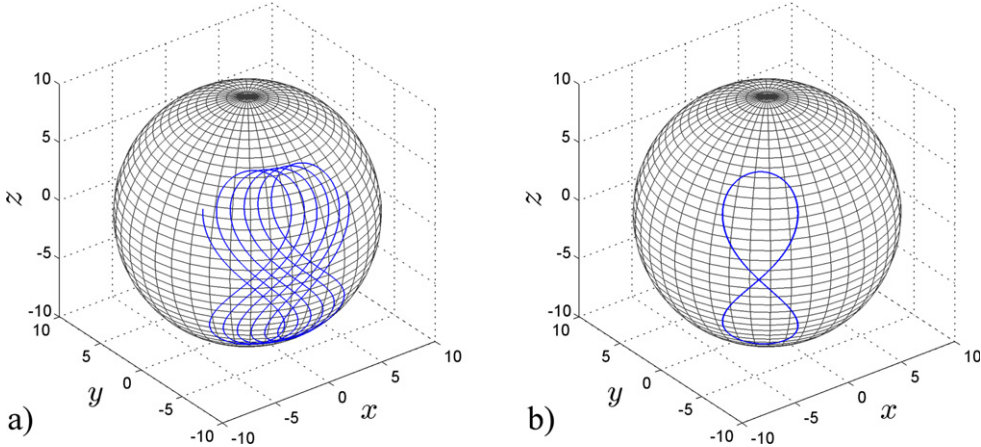


Figure 9. Two different paths where we can see loops in the spherical surface. In (a) we have $p_\varphi = -0.71k$ and we have a drift to the east in the azimuthal motion. In (b) we have $p_\varphi = -0.722k$ and there is no drift, so the trajectory in this case is periodic with an oscillation in the azimuthal angle. In both graphs the initial values are $\theta_0 = \frac{\pi}{3}$ and $p_{\theta 0} = 0.2$ (in arbitrary units). For $p_\varphi < -0.722 k$ the drift would be to the west.

- (i) If $p_\varphi \geq 0$ then $\dot{\varphi}$ is always positive (eastwards in Earth's coordinates).
- (ii) If $p_\varphi < -k$ then $\dot{\varphi}$ is always negative (westwards in Earth's coordinates).
- (iii) If $-k \leq p_\varphi < 0$ then $\dot{\varphi}$ can change its sign according to the variations of θ . Here we have the presence of loops in the trajectory. See figures 8(a)–(c).

Finally, it is important to point out that in the presence of loops, the path could have a drift motion in either east or west directions, depending on the precise numerical value of the constant p_φ , and the path could be like those of the figures 8(a)–(c). In figure 9(a) there is a drift in the eastward direction, and it is possible to find a critical value of p_φ (for the same values of θ_0 and $p_{\theta 0}$), for which there is no drift in the azimuthal motion and the path will be periodic with oscillations back and forth in the angle φ , see figure 9(b). We obtain this critical value of p_φ numerically sweeping over a range of values where we detected a change in the direction of the drift.

7. Conclusions

In this work we studied the dynamics of a charge constrained in a spherical surface, in the field of a magnetic dipole which is located in the centre of the sphere. We followed a Lagrangian formalism within the non-relativistic classical regime. Although the model can no longer be applied to the study of cosmic radiation, we believe that it may illustrate the peculiar dynamics of a point charge in the field of a magnetic dipole. We have not found in the literature the analysis of this restricted Störmer problem. The system has two degrees of freedom and, since the magnetic field of the dipole has an axis of symmetry and the energy is conserved, two constants of motion are readily identified. The nonlinear equations of motion are formally integrable. We analysed the dynamics in the polar angle variable and found the equivalence of this problem with a system with one-dimensional effective potential. We observed that this effective potential has the form of a double well potential with its barrier in

the equator, $\theta = \frac{\pi}{2}$. We discuss different properties of the paths according to this framework. We saw how the maxima and minima which are unstable and stable points respectively, represent horizontal trajectories for which θ is a constant. We described the turning points in the potential in terms of the energy of the system. Then, from the equation of motion in $\dot{\phi}$ we obtain some properties of the path with respect to the azimuthal motion. Here we are predicting the presence of loops in the trajectories, depending on the value of the integration constant given by the conjugate momentum associated with the azimuthal angle. From a numerical integration of the equations of motion, we plotted different graphs to compare them to the analytical results. These graphs include 3D plots of the paths in the spherical surface, and they illustrate the rich variety of trajectories of a charge in the field of a magnetic dipole.

References

- [1] Störmer C 1955 *The Polar Aurora* (Oxford: Clarendon) p 1955
- [2] Sandoval-Vallarta S M 1961 Theory of the geomagnetic effect of cosmic radiation *Encyclopedia of Physics v 9/46/1* (New York: Springer) pp 88–129
- [3] Poincaré H 1896 Remarques sur une expérience de M Birkeland *Comptes Rendus de l'Academie de Sciences* **123** 530–3
- [4] Dragt A J 1965 *Rev. Geophys.* **3** [255–98](#)
- [5] Dragt A J and Finn J M 1976 *J. Geophys. Res.* **81** [2327–40](#)
- [6] de Alcantara Bonfim O F, Griffiths D J and Hinkley S 2000 *Int. J. Bifurcation Chaos* **10** [265](#)
- [7] Jose J V and Saletan E J 2006 *Classical Dynamics: A Contemporary Approach* (New York: Cambridge University Press)
- [8] Goldstein H 1980 *Classical Mechanics* 2nd edn (New York: Addison-Wesley)
- [9] Noether E 1918 Invariante Variationsprobleme *Nachr. D. König. Gesellsch. D. Wiss. Zu Göttingen, Math.-phys. Klasse* **1918** 235–57